

ORIGINAL ARTICLE

Systems Pharmacology Models Can Be Used to Understand Complex Pharmacokinetic-Pharmacodynamic Behavior: An Example Using 5-Lipoxygenase Inhibitors

O Demin¹, T Karelina¹, D Svetlichnyi¹, E Metelkin¹, G Speshilov¹, O Demin Jr¹, D Fairman², PH van der Graaf³ and BM Agoram²

Zileuton, a 5-lipoxygenase (5LO) inhibitor, displays complex pharmacokinetic (PK)-pharmacodynamic (PD) behavior. Available clinical data indicate a lack of dose–bronchodilatory response during initial treatment, with a dose response developing after ~1–2 weeks. We developed a quantitative systems pharmacology (QSP) model to understand the mechanism behind this phenomenon. The model described the release, maturation, and trafficking of eosinophils into the airways, leukotriene synthesis by the 5LO enzyme, leukotriene signaling and bronchodilation, and the PK of zileuton. The model provided a plausible explanation for the two-phase bronchodilatory effect of zileuton—the short-term bronchodilation was due to leukotriene inhibition and the long-term bronchodilation was due to inflammatory cell infiltration blockade. The model also indicated that the theoretical maximum bronchodilation of both 5LO inhibition and leukotriene receptor blockade is likely similar. QSP modeling provided interesting insights into the effects of leukotriene modulation.

CPT: Pharmacometrics & Systems Pharmacology (2013) 2, e74; doi:10.1038/psp.2013.49; published online 11 September 2013

Arachidonic acid (AA) metabolites such as leukotrienes (LT) are key inflammatory mediators, whose overactivity causes bronchoconstriction in asthmatic patients. A number of therapies targeting this pathway are already marketed or in development—montelukast (Singulair; 10 mg once daily (q.d.)), a LTR antagonist and zileuton (Zyflo IR/CR; 600 mg four times a day or 1,200 mg twice a day), a 5-lipoxygenase (5LO) redox enzyme inhibitor, are both marketed agents and 5LO activation protein inhibitors are in development.¹ In spite of extensive clinical experience with this pathway, some gaps in our understanding of this mechanism still exist. For example, the sparse clinical data^{2–4} on the dose response of zileuton is interesting; on acute dosing, both 400 and 600 mg four times a day (q.i.d.) result in similar bronchodilatory response as measured by forced expiratory volume in 1 s (FEV₁); however, when dosing is continued beyond 1–2 weeks, dose response emerges. Also, the relative bronchodilatory potential of different interventions along the AA pathway—e.g., LTR blockade vs. 5LO inhibition vs. 5LO activation protein inhibition is not known. Furthermore, it is not known whether zileuton doses higher than 600 mg q.i.d. would result in even higher efficacy. Understanding these properties would be critical to exploiting the full therapeutic potential of this pathway—for example, to develop a non-redox 5LO inhibitor with less frequent dosing regimen than zileuton (e.g., once daily). An empirical approach such as a pharmacokinetic-pharmacodynamic (PKPD) modeling approach is not suitable for answering these questions; a descriptive model would be unable to provide a mechanistic explanation of the observed PKPD data and a model developed based on 5LO inhibitor data would have limitations in predicting the effects of LTR blockade. Using a quantitative systems pharmacology (QSP) model, we have previously shown⁵ that a non-redox 5LO inhibitor could have the same efficacy as a redox inhibitor.

We further developed this model^{6,7} using literature-published data to help answer these additional questions.

Several mathematical models describing various parts of the 5LO system have already been published.^{8–10} These models describe basic aspects of the enzyme function—binding AA in catalytic and regulatory sites of 5LO and its transformation to products—they do not take into account other important features such as LTA₄ synthesis, reduction of 5-hydroperoxyeicosatetraenoic acid (HPETE) and other peroxides to activate 5LO (pseudoperoxidase reaction), reversible inactivation of 5LO by 5-hydroxyeicosatetraenoic acid,¹¹ and irreversible inactivation by LTA₄.^{12,13} Models of AA metabolism that include both lipoxygenase and cyclooxygenase pathways resulting in formation of LTs and prostanoids have also been reported.^{12,13} The influence of various inhibitors of 5LO and cyclooxygenase on AA metabolism have been studied in these models. However, rate laws for enzymes involved in the AA metabolism have been described in semi-empirical manner using Michaelis–Menten type equations and, consequently, inhibition of 5LO by AA, and activation with product HPETE and pseudoperoxidase activity of 5LO have not been taken into account. Another effort to construct quantitative description of allergic airway inflammation has been performed by Walsh *et al.*¹⁴ The computational model represents Boolean network including eosinophils, T cells, and other cell types as well as a variety of interleukins (IL), and is trained against literature data on C57BL/6 and BALB/c mice. However, this type of modeling does not allow us to understand mechanisms underlying complex PKPD behavior after administration of antiasthmatic drugs.

Therefore, a more detailed model of 5LO system which describes intracellular LT synthesis, extracellular LT transformation, and cell dynamics of eosinophils is required to fully understand the therapeutic potential of this pathway in asthma. This article describes the development and evaluation of such a model.

¹Institute for Systems Biology SPb, Moscow, Russia; ²Clinical Pharmacology, Drug Metabolism, and Pharmacokinetics, MedImmune, LLC, Cambridge, UK; ³Leiden Academic Centre for Drug Research (LACDR), Leiden, Netherlands. Correspondence: BM Agoram (Agoramb@MedImmune.com)

Received 2 January 2013; accepted 18 July 2013; advance online publication 11 September 2013. doi:10.1038/psp.2013.49

RESULTS

In this manuscript, we define the term “5LO system” as a set of processes including intracellular biosynthesis of cysteinyl LT (CysLT) from AA by eosinophils, extracellular transformation of CysLTs, CysLT- and IL-5-mediated eosinophils maturation, migration and activation, production of IL-5 and histamine by eosinophils and mast cells, and effect of CysLTs and histamine on airway smooth muscles contraction. A schematic of the model is presented in **Figure 1**. The model has been developed using data published in literature. These data and some of the key underlying assumptions are presented in **Table 1**. Briefly, the process described by the model is as follows: after maturation in the bone marrow in IL-5-dependent manner, eosinophils migrate to blood, where they are

activated by CysLTs. Activated eosinophils produce CysLTs and IL-5, which further accelerates the process (positive feedback). Both activated and non-activated eosinophils produce histamine. Increase in IL-5 and CysLT blood concentration stimulates migration and accumulation of both activated and non-activated eosinophils to airways. Histamine and CysLT action in the airways results in bronchoconstriction. Zileuton inhibits intracellular production of CysLTs from AA; montelukast inhibits LT binding to its receptor to both activated and non-activated eosinophils and to cause bronchoconstriction.

The systems model describes the complex PKPD behavior of zileuton

To understand the complex PKPD relationship of zileuton observed in the clinic² and to understand the relative efficacy

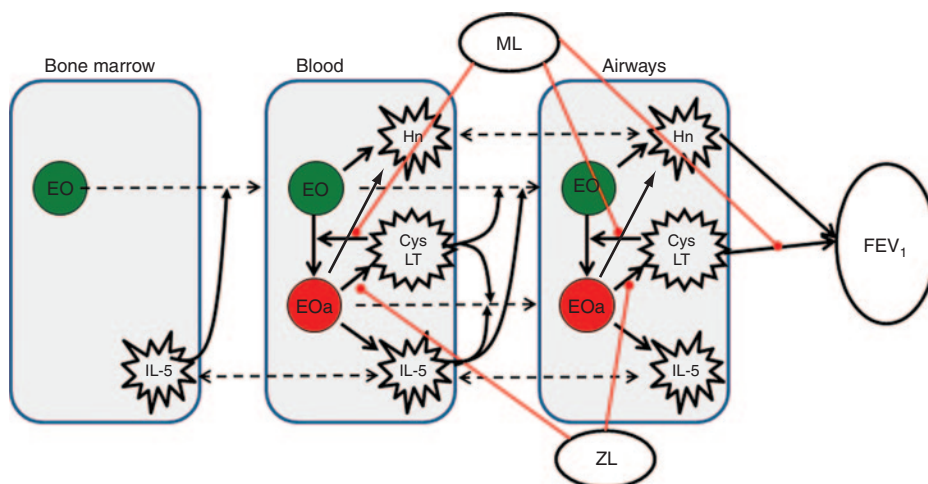


Figure 1 Schematic representation of processes considered in the model. Broken arrows signify transport across tissues. Solid arrows signify production/synthesis/stimulation process. Lines (red) identify points of therapeutic intervention. CysLT, cysteinyl leukotrienes; EO, non-activated eosinophils; EOa, activated eosinophils; FEV₁, forced expiratory volume in 1 s; Hn, histamine; IL-5, interleukin-5; ML, montelukast; ZL, zileuton.

Table 1 Description of available experimental data and facts

| Assumption/fact | References |
|--|-------------|
| Eosinophils and mast cells are the key cells mainly responsible for bronchoconstrictors production | 16,18,44 |
| Cysteinyl leukotrienes C4, D4, and E4 (LTC4, LTD4 and LTE4), histamine, and prostaglandins D2 and F2 are key bronchoconstrictors responsible for excessive bronchoconstriction in asthmatic patients. Among leukotrienes, LTD4 is the strongest bronchoconstrictor | 45 |
| IL-5, granulocyte-macrophage colony-stimulating factor, and stem cell factor are main cytokines governing eosinophils and mast cells maturation | 16,46 |
| Binding of LTD4 and LTC4 to cysteinyl leukotriene receptors 1 and 2 (CysLT1R and CysLT2R) is able to transform inactive eosinophil to activated eosinophil | 44 |
| Only activated eosinophils are responsible for high production of IL-5 and LTC4 | 44 |
| Life span of activated eosinophil is larger than that of inactivated eosinophil | 47 |
| Mast cells are able to produce histamine spontaneously. Mast cells of asthmatics produce more histamine than those of healthy subjects | 16 |
| Eosinophils are able to modulate histamine production in mast cells via excretion of eosinophil cationic protein (ECP). Increase in ECP results in degranulation of mast cells | 16 |
| The key chemoattractants driving eosinophils migration are LTE4 and IL-5 | 31,34,45,48 |
| Increase in LTE4 concentration results in significant accumulation of eosinophils in airways from blood | 18,34,45 |
| Increase in IL-5 blood plasma level leads to elevation of eosinophils trafficking from blood plasma to airways | 31,48 |
| ASM contraction is governed by intracellular calcium level | 45 |
| Intracellular calcium level depends on concentration of bronchoconstrictors (LTD4, LTC4, and histamine) | 49 |
| Binding of LTD4 and LTC4 to CysLT1R and CysLT2R of ASM and binding of histamine to H ₁ receptor results in increase in intracellular Ca ²⁺ concentration | 49,50 |

ASM, airway smooth muscle; IL-5, interleukin-5.

potential of 5LO inhibition vs. LTR inhibition with montelukast, we have simulated 400 and 600 mg q.i.d. zileuton doses and 10 (clinically marketed dose of montelukast as Singulair) and 50 mg montelukast doses q.d. **Figure 2a–c** show the effect of these doses on FEV₁, airway eosinophils and extracellular LT concentrations simulated with our model and clinically measured. These figures show that 5LO inhibition causes bronchodilation in two phases. In the first “acute” phase (0–1 days), bronchodilation is due to direct inhibition of airway LTD4 by ~60% (**Figure 2b**). Minimal changes in airway eosinophils are predicted in this phase (**Figure 2c**). Continued dosing at 400 mg results in equilibrium in the system between the airway eosinophils and the LTD4 and histamine they produce, which in turn attract eosinophils. At higher zileuton doses, the lower levels of LT and histamine achieved in the airways results in an unsustainable cell population in the airways, and hence a continued decrease in the cell numbers and subsequent bronchodilation. A final new steady state corresponding to higher FEV₁ (**Figure 2a**) is reached with low airway cells and LT/histamine concentrations at this higher dose after ~3 weeks of dosing.

Zileuton 600 mg q.i.d. has higher bronchodilation than montelukast 10 mg q.d.

Our simulations indicate that 5LO inhibition with zileuton at 600 mg q.i.d. has higher mean efficacy than LTR inhibition with montelukast at 10 and 50 mg q.d. The maximum FEV₁ increase predicted by the model for zileuton 600 mg is 23% and that for montelukast 10 mg dosing is 5% (**Figure 2a**). Montelukast dosing 10 mg q.d. is predicted to result in essentially unchanged airway cell populations in peripheral tissues (see **Figure 2c** for comparison with clinically measured data) due to low blockade of LT action, similar to that reported by Reiss *et al.*¹⁵ The marginal effect of montelukast on airway cell population (predicted by the model) was found to be due to high competition from airway LT for the CysLT receptors.

Doses of zileuton of 600 mg q.i.d. achieves maximum bronchodilation possible with this mechanism

We also ran simulations to evaluate whether higher doses of zileuton could result in higher efficacy. As shown in **Figure 3a**, 600 mg zileuton q.i.d. results in maximum efficacy. Higher doses result in faster approach to maximum efficacy, but no higher bronchodilation is predicted. Unlike zileuton, higher doses of montelukast are predicted to result in greater efficacy (**Figure 3b**), with doses >250 mg resulting in FEV₁ increases similar to that of zileuton at the higher FEV₁ steady state.

DISCUSSION

We have illustrated how a systems pharmacology modeling approach can be used to understand the complex pharmacological behavior of the 5LO inhibitor zileuton and to compare potential efficacy of intervention at different points along the AA pathway—i.e., 5LO inhibition vs. LTR blockade.

The final model of the 5LO system is an ensemble model of six submodels each describing different aspects of the PKPD system. Each component submodel is a system of ordinary differential equations (ODE), which represent a simplified quantitative representation of the interactions within the

subsystem. For example, the airway trafficking of eosinophils in our model is assumed to be entirely due to IL-5 and LTE₄. However, other cytokines such as granulocyte-macrophage colony-stimulating factor and stem cell factor are also known to be involved in eosinophil maturation, release, and airway trafficking.¹⁶ This is illustrated by the fact that complete inhibition of IL-5 activity reduced lung eosinophilia incompletely by mepolizumab.¹⁷ Similarly, in our model LTs are produced only by eosinophils whereas there is evidence that basophils and mast cells may also be involved in LT production.¹⁶ These important assumptions in our model are made to ensure that only the minimum number of variables is included in our system of equations in order to answer the main questions of interest. Therefore, while each component of the model is quantitative, the overall result should be considered semi-quantitative only. Within these constraints, the model predictions are roughly in line with observations on eosinophil changes observed in the clinic. For example, our model predicts complete reduction in airway eosinophil count at 600 mg q.i.d. dosing of zileuton, whereas Hasday *et al.*¹⁸ reported ~70% reduction in bronchial lavage eosinophils count and preclinical data indicate a maximum reduction in airway eosinophils and CysLT of 80%.¹⁹ For montelukast also, the predicted blood eosinophil reduction is in line with observations; 10% predicted vs. ~10% observed.^{15,20}

Also, it should be noted that in our biophysical model, placebo effects on FEV₁ changes are not accounted for; however, for the sake of qualitative description of bronchodilation by zileuton and to compare the relative effects of 5LO inhibition and LTR blockade, this level of abstraction is sufficient.

All submodel parameters were estimated with adequate precision (**Supplementary Data J** online). Each submodel provided adequate description of the underlying data. The model predicted the two-phase FEV₁ change and the transition time from the first to the second phase after zileuton administration.

Our model provides a plausible explanation for the unusual PKPD behavior of zileuton. In the acute-dosing phase, bronchodilation is achieved by inhibiting LT action on the airways. However, airway eosinophils continue to produce LTs, which continue to attract and activate eosinophils in the airways. Due to the positive feedback in this system, higher level of LT blockade is required to disrupt the trafficking process and therefore, higher doses of zileuton—i.e., doses ≥600 mg—are required to achieve additional bronchodilation. The time required for this additional bronchodilation to be achieved corresponds to the lifespan of activated eosinophils in the airways (3–4 days). Intriguingly, the model suggests that this phenomenon is also true for montelukast, albeit at doses >250 mg q.d., which have not been reported as tested in clinical trials. For montelukast, direct blockade of LTR provides acute bronchodilation; however, competition from high levels of airway LT limits its ability to block eosinophil trafficking, except at doses >250 mg. To the best of the authors' knowledge, this is the first instance of this mechanism being shown to be a plausible explanation of the observed data. Apart from 5LO inhibitors and LTR antagonists, this mechanism is also likely applicable for other anti-inflammatory bronchodilation agents including steroids, which have delayed action.

The model predicts that presently marketed doses of zileuton provide maximum possible bronchodilation available for this

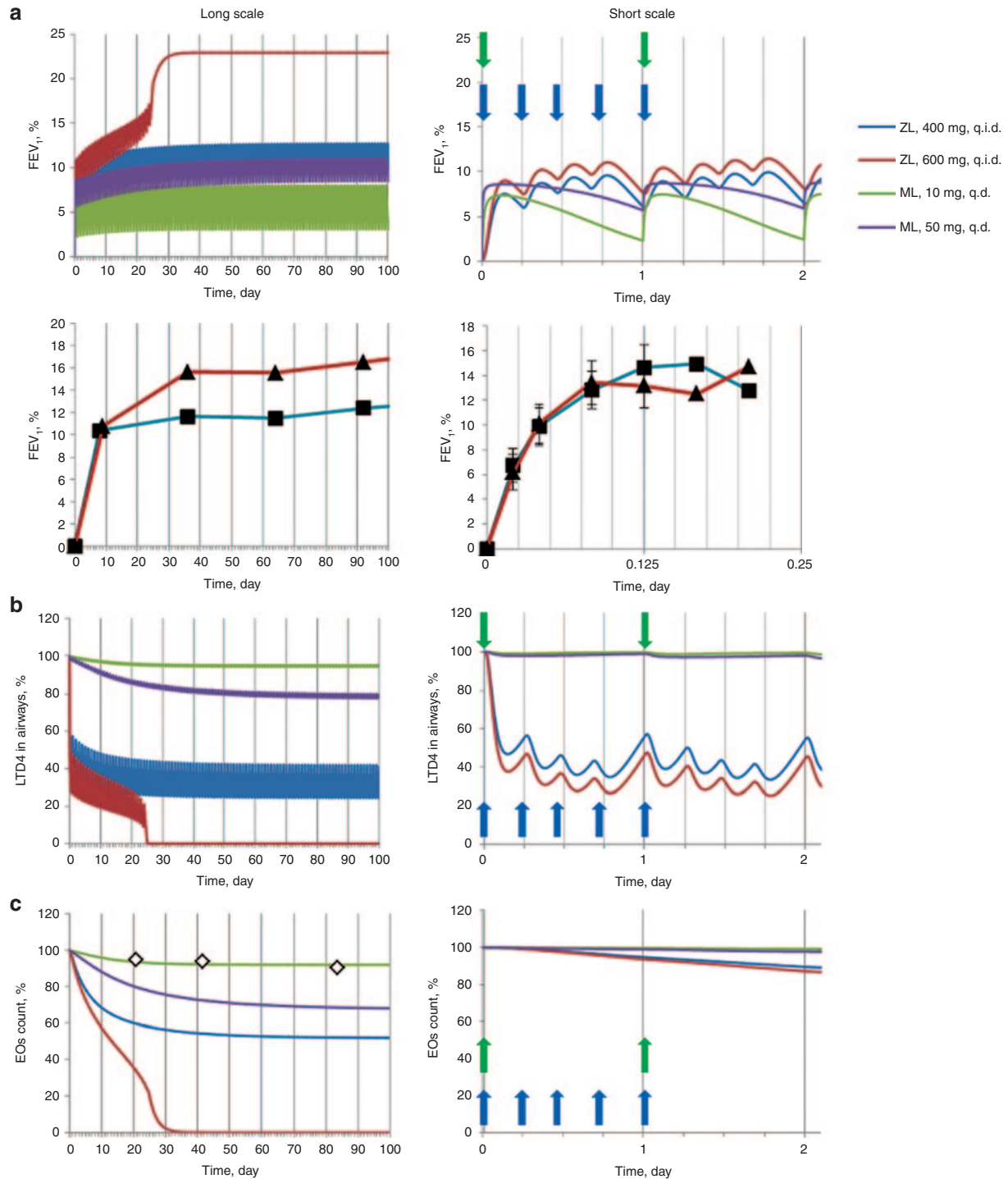


Figure 2 Simulated and clinically measured response to administration of labeled dosages of zileuton (ZL) and montelukast (ML) presented in longer and shorter time scales. Solid lines represent simulations, symbols (squares, triangles, and diamonds) represent clinical observations. Dependence of (a) forced expiratory volume in 1 s (FEV₁), (b) airways LTD4 concentration, and (c) airways eosinophils (EOs) number on time under condition of ZL and ML administration. Four hundred milligrams (blue curve, closed squares) and 600 mg (red curve, closed triangles) of ZL is administered four times a day (q.i.d.); 10 mg (green curve, open diamonds) and 50 mg (violet curve) of ML is administered q.d. All simulated characteristics are expressed as percentage from baseline. Clinically measured data on FEV₁ response to ZL were taken from Liu *et al.*² Vertical blue and green arrows indicate time of administration of ZL during the first day of therapy and ML during two initial days of therapy. q.d., once daily.

mechanism, but those of montelukast only provide bronchodilation due to direct inhibition of LT action. LTR antagonists with greatly improved receptor affinities may provide improved

asthma treatment over montelukast. Our simulations also suggest that at marketed doses, zileuton has higher FEV₁ increase (23%) than montelukast 10 mg (~5%). The predicted

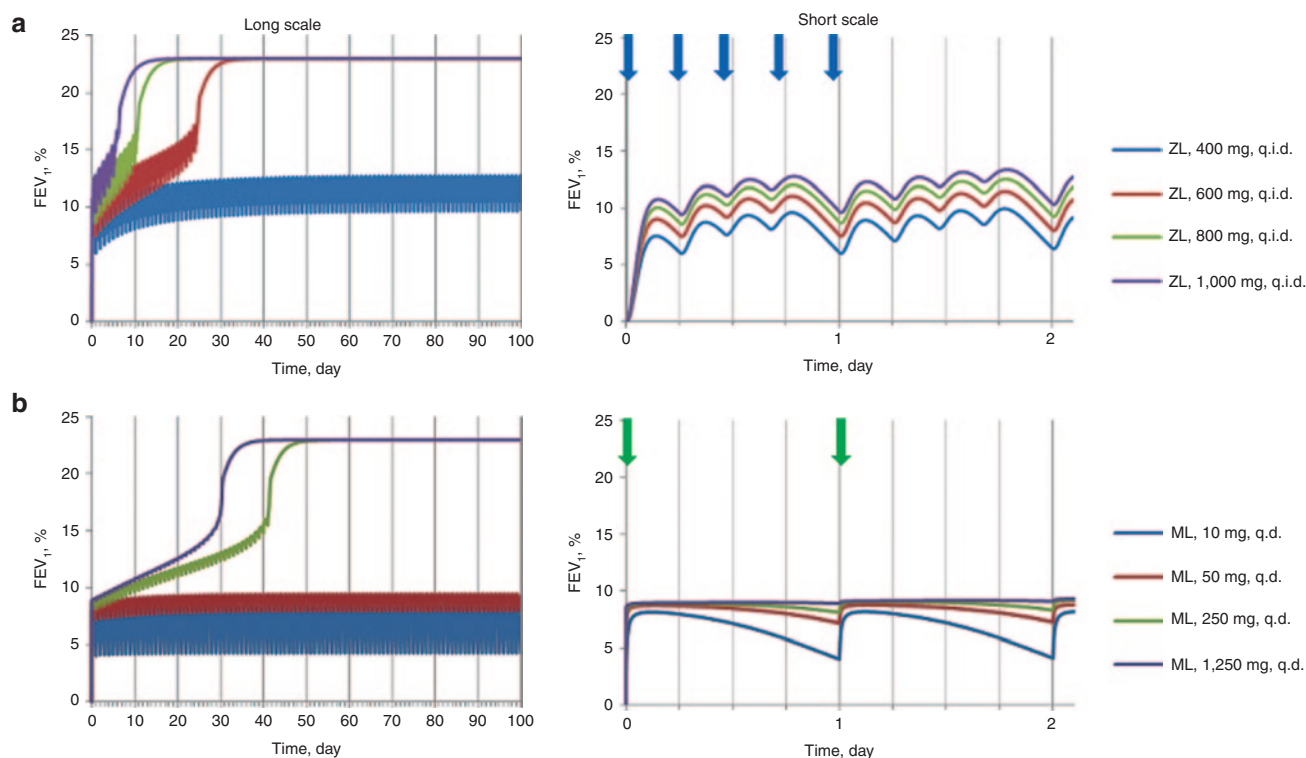


Figure 3 Simulated response to administration of high dosages of zileuton (ZL) and montelukast (ML) presented over chronic and acute time scales. Dependence of FEV₁ (% from baseline) on time under condition of (a) ZL q.i.d. and (b) ML q.d. administration: blue, red, green, and violet curves correspond to 400, 600, 800, 1,000 mg of ZL and 10, 50, 250, 1,250 mg of ML, respectively. Vertical blue and green arrows indicate time of administration of ZL during the first day of therapy and ML during two initial days of therapy, respectively. FEV₁, forced expiratory volume in 1 s; q.d., once daily; q.i.d., four times a day.

effect for montelukast is broadly in line with a meta-analysis,²¹ which indicated bronchodilation in the 5–10% range for montelukast doses of 10–50 mg q.d. Reported bronchodilation for zileuton is lower than predicted^{2–4} (15–20%), presumably due to the assumptions regarding the role of eosinophils as the sole inflammatory cells in the airways. Furthermore, recently Kubavat *et al.*²² have shown in a head-to-head trial that zileuton 1,200 mg twice daily is a more effective bronchodilator (measured by peak expiratory flow rate), than montelukast 10 mg, supporting the model prediction. Therefore, even though the model predictions are semi-quantitative, in the absence of a large database of clinical data, this analysis was able to provide an initial comparison of these two targets' potential efficacy.

The AA system has been extensively studied; hence there are sufficient data in literature to help develop this model. However, for many novel targets, there is often limited information on the link among target modulation, biomarker changes, and ultimate clinical effect. Indeed, this has often been cited as a key reason for not investing in QSP model-based approaches early during drug research and development. Our model suggests that in such situations where mechanistic information is sparse, investment in *in vitro*, *in vivo*, or human tissue assays to generate mechanistic data can provide benefits by enabling such a model-based analysis. This approach is preferable to the often-existing philosophy of running experiments to “confirm” the efficacy of the target in poorly understood animal “disease models”. Development of such mechanistic information to enrich our knowledge of the pathways of

interest should be an important goal of translational research and systems models such as these can provide a quantitative framework for making sense of such complex data.

In conclusion, we have developed a QSP model to help understand the complex behavior of zileuton a 5LO inhibitor. The model provides a number of insights into the AA–LT mechanism causing bronchodilation—it is able to explain the complex PKPD behavior of zileuton; it suggests that zileuton is more efficacious than montelukast at currently marketed doses; it also indicates that improvements in target affinity are more likely to be useful for LTR antagonists than for 5LO inhibition. Our results illustrate how QSP techniques can form a key component of quantitative drug discovery and development strategy.

METHODS

The QSP model of the 5LO system is an ensemble model consisting of six components, describing (i) intracellular LT biosynthesis, (ii) extracellular conversion of LT, (iii) distribution model describing transport of molecules between compartments, (iv) cell dynamics model, (v) biophysical model describing the link between LT levels and bronchial tone, and (vi) PK model. The main stages of model construction are outlined in **Table 2**. The final system of ODEs, experimental facts and assumptions underlying the model structure, rate laws of each process, values of model parameters, and experimental/clinical data used to identify them are presented in **Supplementary Materials** online. The final system consisted

Table 2 Description of stages of model construction

| Step number | Description of step | Type of data used in the step | Parameter identification |
|-------------|--|---|---|
| 1 | Development, verification, and validation of submodel of intracellular LT biosynthesis and mechanism of action of zileuton (presented in details in paper (b1); for brief description see Supplementary Materials (section B) online) | (i) Experimental facts underlying structure of the processes involved in intracellular biosynthesis of LTs and their regulations (ii) <i>In vitro</i> experimental data on kinetics of enzymes involved in intracellular biosynthesis of LTC ₄ (iii) <i>In vivo</i> data on concentration of intracellular metabolites | Most parameter values were taken from previously developed model (b1). Few parameters were fitted to data on intracellular metabolite concentrations |
| 2 | Development and verification of submodel of extracellular conversion of LT (presented in details in Supplementary Materials (section C) online) | (i) Experimental facts underlying structure of the processes involved in extracellular LTs conversion (ii) <i>In vitro</i> experimental data on kinetics of enzymes involved in extracellular conversion of LTs (iii) Human <i>in vivo</i> and <i>ex vivo</i> data on dynamics of LTs conversion (iv) Monkey <i>ex vivo</i> data on dynamics of LTs conversion | Most parameter values were fitted against human and monkey <i>in vivo</i> and <i>ex vivo</i> data. Few parameters were taken from the literature |
| 3 | Development and verification of submodel of distribution describing transport of molecules (LTs, Hn, and IL-5) between compartments (presented in details in Supplementary Materials (section D) online) | (i) Physicochemical properties of the molecules (ii) Physiological properties of the living system (iii) Human <i>in vivo</i> data measured for asthmatic patients | Most parameter values were taken from the literature or calculated on the basis of data available in literature. Parameters responsible for IL-5 distribution between compartments were fitted against human <i>in vivo</i> data |
| 4 | Development, verification, and validation of submodel of the link between LT and histamine levels and bronchial tone (presented in Supplementary Materials (section F) online) | (i) <i>Ex vivo</i> experimental data measured for guinea pigs (ii) Physiological properties of human (iii) Human <i>in vivo</i> data measured for healthy subjects and asthmatic patients | Most parameter values were taken from the literature or calculated/estimated on the basis of data available in literature. Several parameters were identified via fitting against human <i>in vivo</i> data and guinea pigs <i>ex vivo</i> data |
| 5 | Development and verification of the PK submodel describing pharmacokinetics and distribution of zileuton and montelukast (presented in details in Supplementary Materials (section G) online) | (i) Physicochemical properties of zileuton and montelukast (ii) Physiological properties of the living system (iii) Human PK data | Some parameter values were taken from the literature or calculated/estimated on the basis of data available in literature. Several parameters were identified via fitting against human PK data |
| 6 | Development of submodel of cell dynamics (presented in details in Supplementary Materials (section E) online) | Experimental facts underlying structure of the processes and their regulations | |
| 7 | Integration of submodel of cell dynamics with submodels of intracellular LT biosynthesis, extracellular conversion of LT, and submodel of distribution. Identification of parameters of cell dynamics model and parameters responsible for IL-5 transport from airways to blood and to bone marrow (presented in details in Supplementary Materials (section E) online) | (i) <i>Ex vivo</i> data measured for healthy subjects (ii) <i>In vivo</i> experimental data measured for asthmatic patients and healthy subjects | Most parameter values were fitted against <i>ex vivo</i> and <i>in vivo</i> human data. Several parameter values were taken from the literature or calculated/estimated on the basis of data available in literature |
| 8 | Merge of the model obtained at previous stage (stage 7) with the PK submodel and submodel of the link between LT and histamine levels and bronchial tone to form QSP model of 5LO system. Population of the model with data describing volume of tissues and volume of distributions (presented in details in Supplementary Materials (section A) online) | (i) Physicochemical properties of the molecules (ii) Physiological properties of human being | Volumes of tissues were taken from the literature. Volumes of distributions were calculated/estimated on the basis of data available in literature |
| 9 | Validation of QSP model of 5LO system against clinical data | Zileuton and montelukast clinical data | |
| 10 | Simulations/predictions with QSP model of 5LO system | | |

Hn, histamine; IL-5, interleukin-5; LT, leukotrienes; PK, pharmacokinetics; QSP, quantitative systems pharmacology; 5LO, 5-lipoxygenase.

of 33 ODEs, 64 rate laws, and 113 parameters, of which 26 were estimated using literature data and the rest directly taken from literature-reported estimates. Below, we will briefly describe each of the component submodel (i–vi). Submodels (i–iv) are shown in **Supplementary Materials (section A, Figure A1)** online; submodels (v) and (vi) are shown in the **Supplementary Materials (sections F and G)** online.

Submodel of intracellular LT biosynthesis. This submodel represents ODE system describing intracellular LTC₄ biosynthesis from AA. The model includes reactions catalyzed by 5LO, cytosolic phospholipases A₂, glutathione peroxidase, 5-hydroxyicosanoid dehydrogenase, and processes of LTA₄ degradation and LTC₄ excretion from eosinophils located in blood plasma (processes 1–10) and airways interstitium (processes 31–40). Rate laws of the processes and parameter values of the submodel have been taken from Karelina *et al.*⁵ (and references contained therein). Intracellular concentration of LTC₄ in eosinophils of healthy subjects was obtained from Bandeira-Melo *et al.*²³ The ODE system describing intracellular LT biosynthesis, rate equations, and values of parameters are presented in **Supplementary Materials (sections A and B)** online.

Submodel of extracellular conversion of LT. This submodel represents ODE system describing conversion of LTC₄ to LTD₄ and further to LTE₄ catalyzed by γ -glutamyl transpeptidase and dipeptidase located in blood plasma (see processes 11 and 12 in **Supplementary Materials (section A, Figure A1)** online) and airway interstitium (processes 41 and 42), correspondingly. All three CysLTs are exposed to degradation in blood plasma (processes 13–15) and airway interstitium (processes 55–57). Parameters of the model have been identified on the basis of *in vitro* data,²⁴ *ex vivo* experimental data measured for blood of healthy subjects,²⁵ and *in vivo* experimental data (time series of radiolabeled LTs after intravenous infusion) measured for monkey.²⁶ The ODE system describing extracellular conversion of LT, rate equations, and values of parameters are presented in **Supplementary Materials (sections A and C)** online.

Submodel of distribution. This submodel describes transport of LTC₄, LTD₄, LTE₄, and histamine between blood and airway (processes 43, 44, 45, 52), and transport of IL-5 between airway and blood (process 54) and blood and bone marrow (process 28). The submodel describing distribution of the molecules is based on physiologically based PK approach,²⁷ on the one hand, and is simplified as much as possible to meet the compartmental structure of QSP model of 5LO system. All parameters of the submodel can be divided into three groups. First group consists of parameters and those values are calculated on the basis of physicochemical properties of the molecule (for example, tissue partition coefficients, logP, pK_a, etc). Values of the parameters have been taken from literature.^{28,29} Second group includes parameters characterizing physiological properties of the living system (for example, hematocrit, lymph flow rates, blood flow rates, etc). Values of the parameters have been taken from literature.³⁰ Third group includes only two parameters: effective permeability constants of blood to airway and blood to bone marrow transport of IL-5. The values of the parameters have been identified via fitting of the model against *in vivo* data measured in asthmatic patients.³¹ The ODE system

describing distribution of LTC₄, LTD₄, LTE₄, histamine, and IL-5, rate equations, and values of parameters are presented in **Supplementary Materials (sections A and D)** online.

Submodel of cell dynamics. This submodel represents ODE system describing maturation, migration, death, and activation of the eosinophils with LTD₄ and LTC₄ as well as processes associated with the cells such as production/degradation of IL-5 and histamine (see processes 16–27, 29 and 30, 46–51, 53, 58 and 59 in **Supplementary Materials (section A, Figure A1)** online). Parameters of the model have been identified on the basis of the *ex vivo* and *in vivo* experimental data measured for asthmatic patients and healthy subjects.^{18,31–35} ODE system describing cell dynamics of eosinophils, rate equations, and values of parameters are presented in **Supplementary Materials (sections A and E)** online.

Submodel of the link among LT, histamine levels, and bronchial tone. This submodel allows us to couple LTD₄, LTC₄, and histamine concentrations produced by eosinophils with clinically measured endpoint such as FEV₁. The submodel represents several algebraic expressions (**Supplementary Materials (section F)** online) empirically describing level of bronchial smooth muscle contraction as a function of concentration of bronchoconstrictors such as LTD₄, LTC₄, and histamine. Parameters of the model have been identified on the basis of the *ex vivo* experimental data measured for guinea pigs and healthy subjects.^{36–38}

The PK submodel. PK submodel parameters for zileuton and montelukast were estimated using data from refs. 39–41. The plasma PK of zileuton was described by a simple two-compartment model. The plasma PK of montelukast was described by an one-compartment model. It has been assumed that intracellular concentration of zileuton is equal to that of free unbound concentration in plasma or airway interstitium. It has been also assumed that free unbound concentration of montelukast in airway interstitium is equal to that in plasma. The ODE system describing PK of zileuton and montelukast, rate equations, and values of parameters are presented in **Supplementary Materials (sections A and G)** online.

All parameters were estimated using Hooke–Jeeves method implemented in the DBSolve Optimum package (Institute for Systems Biology SPb, Moscow, Russia).⁴² Parameter identification was performed individually for each submodel by fitting to literature data sets pertinent to the part of the system described by the submodel. The 95% confidential intervals were calculated for fitted parameters using method described by Motulsky⁴³ (see **Supplementary Materials** online).

Acknowledgments. We thank Jaime L. Macferrer for discussion of our results and Nail Gizzatkulov for help with calculations. Editor-in-Chief, P.H. van der G. was not involved in the review or decision process for this article.

Author contributions. B.M.A., O.D., and D.F. wrote the manuscript. B.M.A., D.F., and P.H. van der G. designed the research. O.D., T.K., D.S., E.M., G.S., and O.D., Jr. performed the research. O.D., D.S., E.M., G.S., and O.D., Jr. analyzed data. O.D. contributed new reagents/analytical tools.

Conflict of interest. The authors declared no conflict of interest.

Study Highlights

WHAT IS THE CURRENT KNOWLEDGE ON THE TOPIC?

- ✓ The exact mechanism of the two-phase bronchodilatory response of zileuton is not well understood. The comparative efficacy of zileuton and montelukast, both of which act at different points on the arachidonic acid metabolite pathway is also not known.

WHAT QUESTION THIS STUDY ADDRESSED?

- ✓ The study addressed whether application of quantitative systems pharmacology modeling can help characterize the two-phase bronchodilatory response of the 5-lipoxygenase inhibitor zileuton. The comparative efficacy of zileuton and montelukast is also addressed.

WHAT THIS STUDY ADDS TO OUR KNOWLEDGE

- ✓ This study is an example of how modeling can be used within drug discovery to quantitatively “compare” therapeutic targets—especially within the leukotriene cascade.

HOW THIS MIGHT CHANGE CLINICAL PHARMACOLOGY AND THERAPEUTICS

- ✓ This article will encourage more clinical pharmacologists to collaborate with biologists and pharmacologists during target selection by providing a new tool for influencing decisions at this early stage. The eventual outcome of such an involvement would be less clinical attrition and more clinical success.

1. Bain, G. *et al.* Pharmacodynamics and pharmacokinetics of AM103, a novel inhibitor of 5-lipoxygenase-activating protein (FLAP). *Clin. Pharmacol. Ther.* **87**, 437–444 (2010).
2. Liu, M.C., Dubé, L.M. & Lancaster, J. Acute and chronic effects of a 5-lipoxygenase inhibitor in asthma: a 6-month randomized multicenter trial. Zileuton Study Group. *J. Allergy Clin. Immunol.* **98**, 859–871 (1996).
3. Israel, E. *et al.* The effect of inhibition of 5-lipoxygenase by zileuton in mild-to-moderate asthma. *Ann. Intern. Med.* **119**, 1059–1066 (1993).
4. Israel, E., Cohn, J., Dubé, L. & Drazen, J.M. Effect of treatment with zileuton, a 5-lipoxygenase inhibitor, in patients with asthma. A randomized controlled trial. Zileuton Clinical Trial Group. *JAMA* **275**, 931–936 (1996).
5. Karelina, T.A. *et al.* Regulation of leukotriene and 5oxoETE synthesis and the effect of 5-lipoxygenase inhibitors: a mathematical modeling approach. *BMC Syst. Biol.* **6**, 141 (2012).
6. Agoram, B.M. & Demin, O. Integration not isolation: arguing the case for quantitative and systems pharmacology in drug discovery and development. *Drug Discov. Today* **16**, 1031–1036 (2011).
7. van der Graaf, P.H. & Benson, N. Systems pharmacology: bridging systems biology and pharmacokinetics-pharmacodynamics (PKPD) in drug discovery and development. *Pharm. Res.* **28**, 1460–1464 (2011).
8. Aharony, D. & Stein, R.L. Kinetic mechanism of guinea pig neutrophil 5-lipoxygenase. *J. Biol. Chem.* **261**, 11512–11519 (1986).
9. Ludwig, P., Holzhütter, H. & Colosimo, A. Modelling the reaction mechanism of the reticulocyte lipoxygenase. *Biomed. Biochim. Acta* **46**, S241–S244 (1987).
10. Ludwig, P., Holzhütter, H.G., Colosimo, A., Silvestrini, M.C., Schewe, T. & Rapoport, S.M. A kinetic model for lipoxygenases based on experimental data with the lipoxygenase of reticulocytes. *Eur. J. Biochem.* **168**, 325–337 (1987).
11. Aharony, D., Redkar-Brown, D.G., Hubbs, S.J. & Stein, R.L. Kinetic studies on the inactivation of 5-lipoxygenase by 5(S)-hydroperoxyicosatetraenoic acid. *Prostaglandins* **33**, 85–100 (1987).
12. Dobovišek, A., Fajmut, A. & Brumen, M. Role of expression of prostaglandin synthases 1 and 2 and leukotriene C4 synthase in aspirin-intolerant asthma: a theoretical study. *J. Pharmacokinet. Pharmacodyn.* **38**, 261–278 (2011).
13. Yang, K., Ma, W., Liang, H., Ouyang, Q., Tang, C. & Lai, L. Dynamic simulations on the arachidonic acid metabolic network. *PLoS Comput. Biol.* **3**, e55 (2007).
14. Walsh, E.R., Thakar, J., Stokes, K., Huang, F., Albert, R. & August, A. Computational and experimental analysis reveals a requirement for eosinophil-derived IL-13 for the development of allergic airway responses in C57BL/6 mice. *J. Immunol.* **186**, 2936–2949 (2011).
15. Reiss, T.F., Chervinsky, P., Dockhorn, R.J., Shingo, S., Seidenberg, B. & Edwards, T.B. Montelukast, a once-daily leukotriene receptor antagonist, in the treatment of chronic asthma: a multicenter, randomized, double-blind trial. Montelukast Clinical Research Study Group. *Arch. Intern. Med.* **158**, 1213–1220 (1998).
16. Amin, K. The role of mast cells in allergic inflammation. *Respir. Med.* **106**, 9–14 (2012).
17. Pavord, I.D. *et al.* Mepolizumab for severe eosinophilic asthma (DREAM): a multicentre, double-blind, placebo-controlled trial. *Lancet* **380**, 651–659 (2012).
18. Hasday, J.D. *et al.* Anti-inflammatory effects of zileuton in a subpopulation of allergic asthmatics. *Am. J. Respir. Crit. Care Med.* **161**, 1229–1236 (2000).
19. Henderson, W.R. Jr *et al.* The importance of leukotrienes in airway inflammation in a mouse model of asthma. *J. Exp. Med.* **184**, 1483–1494 (1996).
20. Pizzichini, E. *et al.* Montelukast reduces airway eosinophilic inflammation in asthma: a randomized, controlled trial. *Eur. Respir. J.* **14**, 12–18 (1999).
21. Barnes, N. *et al.* Analysis of montelukast in mild persistent asthmatic patients with near-normal lung function. *Respir. Med.* **95**, 379–386 (2001).
22. Kubavat, A.H. *et al.* A randomized, comparative, multicentric clinical trial to assess the efficacy and safety of zileuton extended-release tablets with montelukast sodium tablets in patients suffering from chronic persistent asthma. *Am. J. Ther.* **20**, 154–162 (2013).
23. Bandeira-Melo, C., Woods, L.J., Phoofofo, M. & Weller, P.F. Intracrine cysteinyl leukotriene receptor-mediated signaling of eosinophil vesicular transport-mediated interleukin-4 secretion. *J. Exp. Med.* **196**, 841–850 (2002).
24. Karkowsky, A.M., Bergamini, M.V. & Orłowski, M. Kinetic studies of sheep kidney gamma-glutamyl transpeptidase. *J. Biol. Chem.* **251**, 4736–4743 (1976).
25. Keppler, D. *et al.* Transport and *in vivo* elimination of cysteinyl leukotrienes. *Adv. Enzyme Regul.* **32**, 107–116 (1992).
26. Denzlinger, C., Guhlmann, A., Scheuber, P.H., Wilker, D., Hammer, D.K. & Keppler, D. Metabolism and analysis of cysteinyl leukotrienes in the monkey. *J. Biol. Chem.* **261**, 15601–15606 (1986).
27. Peters, S.A. & Hultin, L. Early identification of drug-induced impairment of gastric emptying through physiologically based pharmacokinetic (PBPK) simulation of plasma concentration-time profiles in rat. *J. Pharmacokinet. Pharmacodyn.* **35**, 1–30 (2008).
28. Rippe, B. & Haraldsson, B. Fluid and protein fluxes across small and large pores in the microvasculature. Application of two-pore equations. *Acta Physiol. Scand.* **131**, 411–428 (1987).
29. Rodgers, T. & Rowland, M. Physiologically based pharmacokinetic modelling 2: predicting the tissue distribution of acids, very weak bases, neutrals and zwitterions. *J. Pharm. Sci.* **95**, 1238–1257 (2006).
30. Baxter, L.T., Zhu, H., Mackensen, D.G. & Jain, R.K. Physiologically based pharmacokinetic model for specific and nonspecific monoclonal antibodies and fragments in normal tissues and human tumor xenografts in nude mice. *Cancer Res.* **54**, 1517–1528 (1994).
31. Stirling, R.G., van Rensen, E.L., Barnes, P.J. & Chung, K.F. Interleukin-5 induces CD34(+) eosinophil progenitor mobilization and eosinophil CCR3 expression in asthma. *Am. J. Respir. Crit. Care Med.* **164**, 1403–1409 (2001).
32. Chavis, C. *et al.* Leukotriene E4 plasma levels in adult asthmatic patients with variable disease severity. *Allergy* **52**, 589–592 (1997).
33. Corhay, J.L., Bury, T., Louis, R. & Radermecker, M.F. Plasma histamine and bronchial reactivity in allergic asthma. *Allergy* **48**, 547–549 (1993).
34. Laitinen, L.A., Laitinen, A., Haahtela, T., Viikka, V., Spur, B.W. & Lee, T.H. Leukotriene E4 and granulocytic infiltration into asthmatic airways. *Lancet* **341**, 989–990 (1993).
35. Shindo, K., Matsumoto, Y., Sumitomo, M., Matsumura, M. & Okubo, T. Measurement of leukotriene C4 and D4 in arterial blood of asthmatic patients during remission. *Ann. Allergy* **66**, 405–410 (1991).
36. Amrani, Y., Moore, P.E., Hoffman, R., Shore, S.A. & Panettieri, R.A. Jr. Interferon-gamma modulates cysteinyl leukotriene receptor-1 expression and function in human airway myocytes. *Am. J. Respir. Crit. Care Med.* **164**, 2098–2101 (2001).
37. Kanaoka, Y. & Boyce, J.A. Cysteinyl leukotrienes and their receptors: cellular distribution and function in immune and inflammatory responses. *J. Immunol.* **173**, 1503–1510 (2004).
38. Morishima, H., Kajiwara, K., Akiyama, K. & Yanagihara, Y. Ligation of Toll-like receptor 3 differentially regulates M2 and M3 muscarinic receptor expression and function in human airway smooth muscle cells. *Int. Arch. Allergy Immunol.* **145**, 163–174 (2008).

39. Awni, W.M. *et al.* Pharmacokinetics of zileuton and its metabolites in patients with renal impairment. *J. Clin. Pharmacol.* **37**, 395–404 (1997).
40. Wong, S.L., Awni, W.M., Cavanaugh, J.H., el-Shourbagy, T., Locke, C.S. & Dubé, L.M. The pharmacokinetics of single oral doses of zileuton 200 to 800mg, its enantiomers, and its metabolites, in normal healthy volunteers. *Clin. Pharmacokinet.* **29** (suppl. 2), 9–21 (1995).
41. Zhao, J.J. *et al.* Pharmacokinetics and bioavailability of montelukast sodium (MK-0476) in healthy young and elderly volunteers. *Biopharm. Drug Dispos.* **18**, 769–777 (1997).
42. Gizzatkulov, N.M., Goryanin, I.I., Metelkin, E.A., Mogilevskaya, E.A., Peskov, K.V. & Demin, O.V. DBSolve Optimum: a software package for kinetic modeling which allows dynamic visualization of simulation results. *BMC Syst. Biol.* **4**, 109 (2010).
43. Motulsky, H.J. & Christopoulos, A. *Fitting Models to Biological Data Using Linear and Nonlinear Regression. A Practical Guide to Curve Fitting* (GraphPad Software Inc, San Diego, 2003).
44. Bandeira-Melo, C. & Weller, P.F. Eosinophils and cysteinyl leukotrienes. *Prostaglandins Leukot. Essent. Fatty Acids* **69**, 135–143 (2003).
45. Gauvreau, G.M., Parameswaran, K.N., Watson, R.M. & O'Byrne, P.M. Inhaled leukotriene E(4), but not leukotriene D(4), increased airway inflammatory cells in subjects with atopic asthma. *Am. J. Respir. Crit. Care Med.* **164**, 1495–1500 (2001).
46. Clutterbuck, E.J., Hirst, E.M. & Sanderson, C.J. Human interleukin-5 (IL-5) regulates the production of eosinophils in human bone marrow cultures: comparison and interaction with IL-1, IL-3, IL-6, and GM-CSF. *Blood* **73**, 1504–1512 (1989).
47. Lee, E., Robertson, T., Smith, J. & Kilfeather, S. Leukotriene receptor antagonists and synthesis inhibitors reverse survival in eosinophils of asthmatic individuals. *Am. J. Respir. Crit. Care Med.* **161**, 1881–1886 (2000).
48. Palframan, R.T., Collins, P.D., Severs, N.J., Rothery, S., Williams, T.J. & Rankin, S.M. Mechanisms of acute eosinophil mobilization from the bone marrow stimulated by interleukin 5: the role of specific adhesion molecules and phosphatidylinositol 3-kinase. *J. Exp. Med.* **188**, 1621–1632 (1998).
49. Dumitriu, D., Prié, S., Bernier, S.G., Guillemette, G. & Sirois, P. Mechanism of action of leukotriene D4 on guinea pig tracheal smooth muscle cells: roles of Ca⁺⁺ influx and intracellular Ca⁺⁺ release. *J. Pharmacol. Exp. Ther.* **280**, 1357–1365 (1997).
50. Accomazzo, M.R. *et al.* Leukotriene D4-induced activation of smooth-muscle cells from human bronchi is partly Ca²⁺-independent. *Am. J. Respir. Crit. Care Med.* **163**, 266–272 (2001).



CPT: Pharmacometrics & Systems Pharmacology is an open-access journal published by Nature Publishing Group. This work is licensed under a Creative Commons Attribution-NonCommercial-NoDerivatives Works 3.0 License. To view a copy of this license, visit <http://creativecommons.org/licenses/by-nc-nd/3.0/>

Supplementary information accompanies this paper on the *CPT: Pharmacometrics & Systems Pharmacology* website (<http://www.nature.com/psp>)